

CASE REPORT

Companion or pet animals

Computed tomographic, ultrasonographic, MRI and radiographic findings of a venous malformation with phleboliths in the thoracic limb of a dog

Kevin Kang¹  | Robert M. Kirberger²  | Giselle Hosgood³  | Nerissa Stander⁴ 

¹Diagnostic Imaging Department, School of Veterinary Medicine, Murdoch University, Perth, Western Australia, Australia

²Department of Companion Animal Clinical Studies, Faculty of Veterinary Science, University of Pretoria, Pretoria, South Africa

³Small Animal Surgery Department, School of Veterinary Medicine, Murdoch University, Perth, Western Australia, Australia

⁴Vet Imaging Specialists, The Animal Hospital, Murdoch University, Perth, Western Australia, Australia

Correspondence

Kevin Kang, School of Veterinary Medicine, Murdoch University, South Street Campus, 90 South Street, Murdoch, Western Australia 6150, Australia.
Email: kevin.kang@murdoch.edu.au

[Correction added on 29 March 2022, after first online publication: The Acknowledgement section was updated.]

Abstract

An 11-month-old entire male Rottweiler was referred for further investigation of raised, soft, compressible, non-pulsatile, subcutaneous tubular structures along the right antebrachium that had been diagnosed to be a vascular malformation on histopathology of a subcutaneous biopsy. Computed tomographic (CT) with angiography did not reveal an arteriovenous malformation or fistula. Ultrasonography of the limb demonstrated a venous malformation with thrombi and phleboliths. An MRI study of the limb was consistent with a venous malformation with small rounded luminal signal voids that were confirmed to be phleboliths. Radiography at follow-up demonstrated phleboliths. This is the first report describing the combined CT, ultrasonographic, MRI and radiographic characteristics of venous malformation with phleboliths in a limb of a dog.

BACKGROUND

Peripheral venous malformation is rarely reported in dogs, with only a single case report involving the pelvic limb of a 6-year-old dog.¹ In people, venous malformations are common with 40% of lesions occurring in the extremities, 40% in the head and neck region and 20% in the trunk.² The International Society for the Study of Vascular Anomalies classifies venous malformations as a subdivision of vascular malformations, which are non-neoplastic lesions present at birth and grow in proportion with the subject, and do not regress.³ Venous malformations can occur in any tissue, including the skin, muscle, bone and joints.⁴

Localised intravascular coagulopathy occurs in almost 60% of people with venous malformations.⁵ The resultant thrombi may calcify to form stone-like structures called phleboliths, which are considered a characteristic feature of venous malformations.^{4,6,7} Calcium phosphate and calcium carbonate are deposited at the centre of the thrombus, and calcification progresses from the inner layer towards the periphery.⁸ Fibrosis develops progressively on the surface of the calcified thrombus in a laminar pattern and also undergoes calcification.⁸ The repetition of this process results in a

laminated pattern as the phlebolith increases in size.⁸ Phleboliths can demonstrate individual variation in their size and structure, and the core and the cortex of a phlebolith may be made up of varied grades of calcification.⁸ Histologically, phleboliths are calculi with characteristic concentric lamination.⁹ Phleboliths have not been reported in the veterinary literature. However, a thrombosed orbital venous malformation (varix) has been reported in a dog.¹⁰

This case details the first report of a venous malformation with phleboliths in a limb of a dog and the application of different imaging modalities to confirm the diagnosis.

CASE PRESENTATION

An 11-month-old, entire male Rottweiler was referred to the Small Animal Surgery Department at The Animal Hospital, Murdoch University, for further assessment of a suspected vascular malformation of the right thoracic limb. Multiple, subcutaneous tubular swellings had reportedly been present, extending from the elbow to the carpus, since the dog was 7 months old. The referring veterinarian initially treated the dog with non-steroidal anti-inflammatories (drug and dosage unknown) and later amoxicillin/clavulanic acid (13.1 mg/kg

This is an open access article under the terms of the [Creative Commons Attribution-NonCommercial-NoDerivs](https://creativecommons.org/licenses/by-nc-nd/4.0/) License, which permits use and distribution in any medium, provided the original work is properly cited, the use is non-commercial and no modifications or adaptations are made.

© 2022 The Authors. *Veterinary Record Case Reports* published by John Wiley & Sons Ltd on behalf of British Veterinary Association.

PO every 12 hours, Amoxycylav, Apex Laboratories) and metronidazole (10.5 mg/kg PO every 12 hours, Metronide, Sanofi-Aventis Australia) without any improvement. Subsequently, a focal subcutaneous area of the affected region was biopsied by the referring veterinarian, and histopathology identified large ectatic and variably sized blood vessels mainly lined by flat endothelial cells. Within some sections, blood vessels contained well-organised fibrin thrombi with moderate degrees of encapsulating fibrosis and central areas of mineralisation. The histopathologic diagnosis was vascular malformation with multifocal fibrin thrombi.

On clinical examination at the time of referral, there were raised, soft, compressible, non-pulsatile, subcutaneous tubular structures along the length of the medial and lateral aspect of the right antebrachium. The most distended tubular structures were located at the proximomedial aspect of the limb from the elbow extending distally for 15 cm. The affected antebrachium was circumferentially larger than the contralateral thoracic limb, but the dog did not exhibit lameness or pain on palpation of the limb.

INVESTIGATIONS

Initially, the vascular malformation diagnosed on histopathology was interpreted by our clinicians to be an arteriovenous malformation or arteriovenous fistula. Helical CT angiography was performed (Siemens Somatom Emotion 16-Slice, Siemens Healthcare) to assist with treatment planning. The dog was anaesthetised and positioned in sternal recumbency with the thoracic limbs extended cranially. Image acquisition parameters consisted of 1.5 mm thick transverse images, pitch 0.8, tube rotation time of 0.6 seconds, 130 kV and 160 mAs. Limb images were acquired using soft tissue (window width = 350 Hounsfield units (HU), window level = 40 HU) and bone algorithms (window width = 2000 HU, window level = 450 HU). Intravenous contrast (iohexol, Omnipaque 300 mg I/ml, GE Healthcare) was administered into the left cephalic vein at 2 ml/kg with a pressure injection (Apollo Single Injector APO 100, APOLLO RT) over 30 seconds (2 ml/s at 60 psi). The arterial phase scan began 15 seconds from the start of contrast administration, followed by delayed phases at 45 and 75 seconds. CT identified a soft tissue swelling of variable thickness (up to 2 cm) in the subcutis of the caudomedial aspect of the right distal antebrachium (Figure 1a–c). There was normal arterial supply and venous drainage to the limb. A small area of mineralisation (up to 401 HU), measuring 4.3 mm in diameter was identified proximal to the olecranon and initially thought to be the biopsy site (Figure 1a–c). The CT ruled out an arteriovenous malformation or arteriovenous fistula but failed to demonstrate a reason for the superficial swellings.

Following CT, ultrasonography of the limb (GE Logiq S8, GE Healthcare) generated B-mode and colour Doppler images of the antebrachium in sagittal and transverse planes using a 2–8 MHz (9L-D, GE Healthcare) and 4–15 MHz (L8-18i-D, GE Healthcare) linear array transducers. Multiple compressible thin-walled, tortuous, tubular, dilated anechoic structures, suggestive of vessels were identified. Within these vessels were rounded hypoechoic foci, measuring up to 12.3 mm in length and 5.3 mm in thickness, consistent with thrombi. Some of these foci contained a poorly shadowing hyperechoic centre

LEARNING POINTS/TAKE HOME MESSAGES

- The presence of phleboliths in a vascular malformation is diagnostic for venous malformation.
- Ultrasonography allows real-time assessment of flow dynamics (low-flow vs. high-flow) within the vascular malformation and detection of the varying stages of phlebolith formation.
- In people, MRI is the imaging modality of choice for the diagnosis of venous malformations, which has a characteristic MRI appearance.
- CT with angiography can exclude high-flow vascular malformations and demonstrate phleboliths.
- Radiography can screen for the presence of phleboliths.

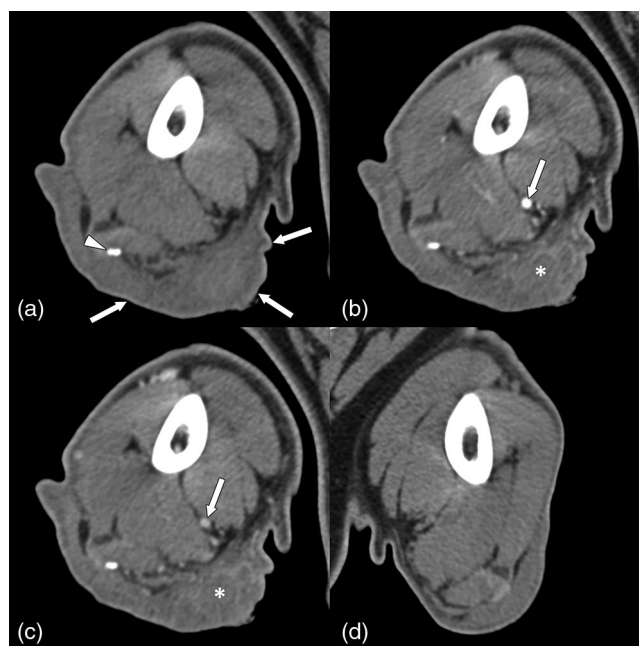


FIGURE 1 Transverse soft tissue window CT images of the right distal brachium—(a) survey image, (b) arterial phase, (c) delayed phase—and left distal brachium—(d) survey image—at the same level. (a) The soft tissue swelling at the caudomedial aspect of the right distal brachium (white arrows) and the phlebolith (up to 401 Hounsfield units [HU]) that was initially thought to be the previous biopsy site (white arrowhead). (b) Enhancement of a normal artery during the arterial phase (white arrow). Round mildly hypoattenuating areas within the soft tissue swelling (*). (c) The same artery during the delayed phase (white arrow) and hypoattenuating areas peripherally slightly enhanced (*). (d) The normal left distal brachium for comparison of soft tissue swelling

with a mildly coarse echotexture, suggestive of minor calcification (possible early phlebolith formation) or area of fibrosis within the thrombi (Figure 2a,b). Colour and power Doppler analysis could not demonstrate flow within the vessels, but smaller more vascularised vessels were seen interdigitating the dilated vessels (Figure 2b). The ultrasonographic findings were suggestive of a low-flow vascular malformation, and the presence of possible phleboliths was characteristic of a venous malformation.

Ten days later, an MRI of the right distal humerus to the mid-metacarpal region was performed using a 1.5 Tesla

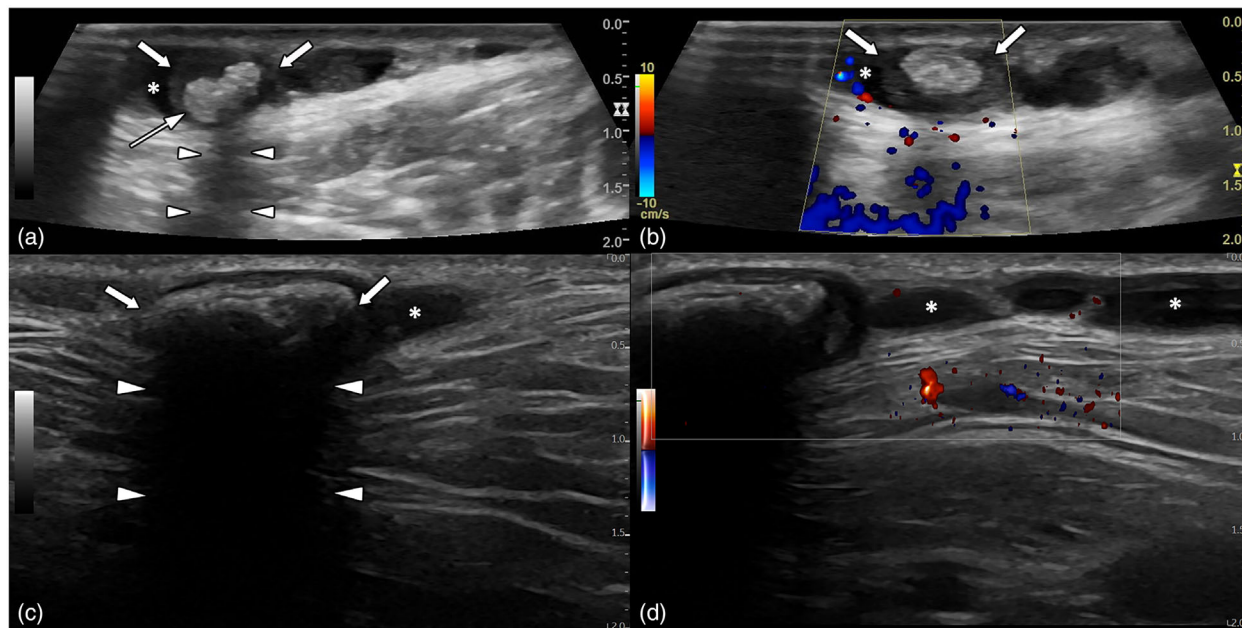


FIGURE 2 Ultrasound images of the right antebrachium (a and b, initial ultrasound examination; c and d, ultrasound examination 29 months later). (a) B-mode image. Within a dilated malformed vessel (*) there is a thrombus (white arrows) with a suspected calcified core (early phlebolith formation) or area of fibrosis (thin white arrow) casting a weak distal acoustic shadowing artefact (white arrowheads). (b) Colour Doppler image. Flow could not be demonstrated within the lumen of the malformed vessel that contains a calcified thrombus (phlebolith; white arrows) but identified small interdigitating vessels and flow in the soft tissues adjacent to the malformed vessel (*). (c) B-mode image. Within a dilated malformed vessel (*) at the level of the firm palpable lesion noted on examination 29 months later, there is a phlebolith (white arrows) casting a marked distal acoustic shadow (arrowheads). (d) Colour Doppler image. Flow could not be demonstrated within the lumen of the malformed vessels (*) that contains a phlebolith

MRI unit (GE Signa Excite, GE Healthcare) to confirm and characterise the venous malformation and the extent of tissue involvement. The study comprised T2-weighted (repetition time [TR] 3176 ms, echo time [TE] 83.712–89.136 ms) and pre- and postcontrast T1-weighted images in sagittal and transverse planes (TR 1509–2360 ms, TE 9.408–10.488 ms). Proton-density (PD)-weighted spin-echo (SE) images in transverse and dorsal planes (TR 3025–5263 ms, TE 39.22–42.304 ms) and postcontrast T1-weighted three-dimensional fat-suppressed images (TR 13.473 ms, TE 6.764 ms) were also obtained. The slice thickness was 3.0 mm, and the interslice spacing was 3.5 mm. Intravenous gadolinium-based contrast agent (gadobutrol 1 mmol/ml, Gadovist 1.0, Bayer Australia) was given at 0.2 ml/kg.

The MRI identified multiple tubular thin-walled, tortuous structures, ranging in size from 1 to 14 mm in diameter, extending along the subcutaneous region of the right antebrachium (Figure 3a–c). These structures spanned the entire scan field of view from the level of the distal third of the humerus to the mid-metacarpal region, although tapered significantly in magnitude towards the periphery of the scan. These tortuous structures did not radiate from a central nidus and were haphazardly aligned with the long axis of the limb, extending circumferentially along the limb. There was no appreciable extension into the deeper fascial planes or underlying musculature. On T1-weighted imaging, the structures were of low signal intensity compared with fat and high signal intensity compared with skeletal muscle. On T2 and PD-weighted imaging, the structures were strikingly hyperintense compared with fat and skeletal muscle (Figure 3b). Within some of the tortuous vessels at the level of the craniomedial aspect of the elbow, there were well-defined rounded

intraluminal signal voids on all pulse sequences, measuring up to 8 mm in diameter, indicative of mineral, and thus phleboliths (Figure 3c,d). Following contrast administration, there was a mild delayed enhancement of the tortuous vessels within which tiny, more strikingly enhancing, venous tributaries of the cephalic and accessory cephalic vein interdigitated. Overall, the large superficial veins of the thoracic limb were considered within normal limits for size, and there were no arterial abnormalities detected. The MRI findings were consistent with a superficial venous malformation with phleboliths.

Retrospective scrutiny of the CT study identified several small mineral attenuating (174–655 HU) structures ranging in size from 1.8 to 4.6 mm in diameter that were distant from the known biopsy site at the medial aspect of the proximal antebrachium. These corresponded to the intraluminal signal voids seen on the MRI images (Figure 3e), confirming that the signal voids were phleboliths. Additionally, a re-examination of the affected area revealed subtle slightly hypoattenuating circular areas, up to 7 mm in diameter, which enhanced slightly at the periphery after contrast administration (Figure 1b,c), compatible with non-enhancing vessel content.

DIFFERENTIAL DIAGNOSIS

The imaging findings were consistent with a superficial venous malformation with phleboliths. Retrospectively, the initial diagnoses of a peripheral arteriovenous malformation or arteriovenous fistula, although still potential differential diagnoses, should not have been considered due to the non-pulsatile nature of the vascular lesions.

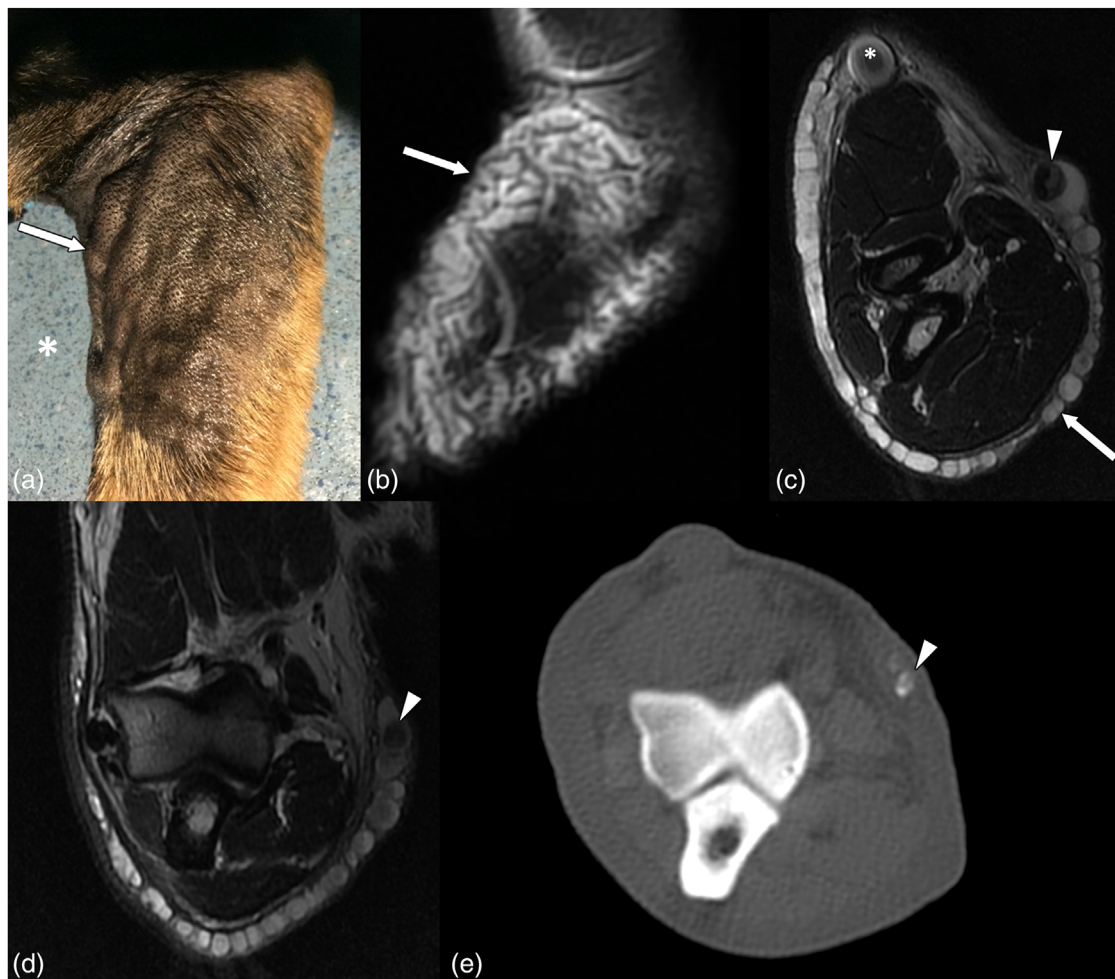


FIGURE 3 Anatomic, MRI and CT images of the right antebrachium. (a) Multiple superficial tortuous blood vessels (white arrow) on the medial aspect of the right proximal antebrachium. The white asterisk denotes the cranial aspect. (b) Sagittal T2-weighted MRI image of the right proximal antebrachium at the level of (a) demonstrating multiple tortuous structures (white arrow) that are hyperintense compared to fat and skeletal muscle, typical of venous malformations. (c) Transverse T2-weighted MRI image of the right antebrachium distal to the elbow joint demonstrating the venous malformation extending along the subcutaneous region (white arrow) and occupying the entire caudal aspect of the visible antebrachium and clearly delineated from the underlying musculature. A phlebolith is seen as a well-defined round area of the signal void within a vascular channel (white arrowhead). Normal blood flow within the cephalic vein appears as a signal loss on spin-echo sequences due to time-of-flight effects (white asterisk). (d) Transverse T2-weighted MRI image of the right antebrachium at the level of the elbow joint demonstrating a phlebolith seen as a well-defined rounded area of the signal void within a vascular channel (white arrowhead). (e) Transverse precontrast bone algorithm CT image at the same level as the image in (d) demonstrating a mineral attenuating round structure (up to 655 HU) (white arrowhead), which correlates to the signal void of the phlebolith seen in (d)

TREATMENT OUTCOME AND FOLLOW-UP

The dog was discharged with no treatment, and the owner was warned of the possibility of the lesion progressing and eventually requiring intervention. Twenty-nine months later the dog was returned for reassessment. The dog was reported to be clinically well except for one episode of a transient increase in swelling with lameness after swimming. On re-examination, the limb appeared similar to the initial presentation. However, there was a palpable, approximately 12 mm diameter, round, firm, mildly irregularly marginated subcutaneous nodule craniomedial to the right elbow joint that was not present previously (Figure 4a).

Repeat ultrasonography (GE Logiq E10s, GE Healthcare) of the right antebrachium generated B-mode and multi-modal Doppler images using a 4–15 MHz linear array transducer (ML6-15, GE Healthcare). The venous malformation was unchanged. At the level of the subcutaneous nodule, an 11.4 mm long and 8.6 mm wide, ovoid, well-defined,

mildly irregularly marginated hyperechoic focus that exhibited marked distal acoustic shadowing within a dilated vessel was identified, consistent with a phlebolith (Figure 2c). Several smaller phleboliths and multiple thrombi were seen, and multi-modal Doppler analysis could still not demonstrate flow within the vessels (Figure 2d).

A mediolateral radiograph of the right antebrachium (Varian Medical Systems, Varian Interay) using an Agfa DR console (DX-D 40C, AGFA Healthcare) with exposure factors of 60 kV and 4 mAs showed multifocal to diffuse poorly defined increased soft tissue opacity, especially on the caudal aspect of the antebrachium, corresponding to the diffuse venous malformation (Figure 4b). Cranial to the proximal radius, there was a 12 mm long and 8.8 mm thick, ovoid, well-defined structure of heterogeneous mineral opacity that displayed a lamellated pattern with a non-uniform mineral centre, consistent with a phlebolith (Figure 4b). This phlebolith corresponded to the palpable firm subcutaneous lesion that was identified as a large phlebolith on ultrasound.

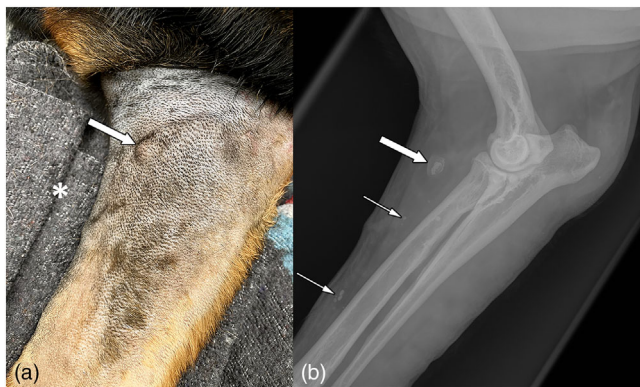


FIGURE 4 Anatomic and mediolateral radiograph of the right antebrachium. (a) Palpable firm subcutaneous nodule craniomedial to the right elbow joint (white arrow). The white asterisk denotes the cranial aspect. (b) Mediolateral radiograph of the right antebrachium. A large phlebolith with a characteristic laminated morphology and non-uniform mineral core is seen at the same level as the palpable firm subcutaneous nodule (thick white arrow). Multiple smaller phleboliths with a homogeneous mineral opacity are also seen distally (thin white arrows)

Further distally, there were additional multiple, small (1 mm to 3 mm diameter), round to ovoid, well-defined smoothly margined foci of uniform mineral opacity in the soft tissues, consistent with smaller phleboliths (Figure 4b).

DISCUSSION

This report describes the CT, ultrasonographic, MRI, and radiographic characteristics of venous malformation with phleboliths in a limb of a dog. Venous malformations are characterised as low-flow abnormal collections of veins with variable luminal sizes and wall thickness.⁴ Histologically, venous malformations have irregular, variably dilated or thickened dysplastic-appearing vascular channels lined with flat mature endothelial cells as seen in our case.¹¹ Although phleboliths were detected on imaging studies, the biopsy in our case was performed by the referring veterinarian prior to referral without knowledge of venous malformations and phleboliths. The biopsy site may not have targeted a region with mature phleboliths, and therefore phleboliths were not detected histologically. In people, some venous malformations may not be evident until later in childhood or young adulthood, as the period of greatest enlargement occurs from infancy to puberty as was the case in our dog.²

In the present case, findings on multiple imaging modalities are described to offer complementary characterisation of the venous malformation with phleboliths. In people, distinguishing between a low-flow (venous or lymphatic malformations) and a high-flow vascular malformation (arteriovenous malformations or arteriovenous fistulas) is critical because the treatment options are different.¹² Ultrasonography is therefore the recommended initial imaging modality in people to help differentiate low-flow from high-flow vascular malformations.^{13,14} Phleboliths are observed in venous malformations^{4,6-8,15,16} and when present in a vascular malformation, aid in the diagnosis of venous malformation.¹⁵ Sonographically, phleboliths are described as solitary or multiple variable-sized hyperechoic foci with distal acoustic shadowing artefacts.^{15,16} The initial ultrasound examination

identified hypoechoic foci within dilated blood vessels that exhibited a poorly shadowing hyperechoic core that was suspected to be minor calcification of thrombi. This sonographic appearance could be attributed to the calcification process that begins from the centre of the thrombus.⁸ Additionally, the core of a phlebolith may consist of varied grades of calcification.⁸ The degree of hyperechogenicity and distal acoustic shadowing of the evolving phleboliths seen on the initial ultrasound examination and the recheck 29 months later may represent the sonographic appearance of the evolutionary progression of phleboliths. Interestingly, at the recheck 29 months later, although the large phlebolith was moderately mineral opaque with a laminated appearance on radiographs, it did not exhibit a strongly hyperechoic curvilinear interface on ultrasonography as would be expected from a mineral structure despite the marked distal acoustic shadowing artefact.

Doppler analysis did not demonstrate flow within the abnormal vessels, which is reported in a minority of venous malformations, and is consistent with thrombosis and the presence of phleboliths in the venous malformations.¹⁵ In the absence of phleboliths, venous malformations can be easily differentiated from macrocystic lymphatic malformations on ultrasonography because the latter appear as enlarged cystic spaces that are often multiseptated and may contain dependent echogenic debris.^{3,14} However, microcystic lymphatic malformations can be challenging to differentiate from venous malformations because the cystic spaces are smaller, and there may not be a visible cystic component.¹⁴

MRI is the modality of choice for the confirmation, characterisation and differentiation of vascular malformations in people.¹³ The MRI from this dog defined the full extent of the venous malformation and the lack of involvement of adjacent structures, critical for potential therapy planning.¹⁷ Our case demonstrated many of the MRI characteristics of venous malformations previously described.^{2,10,17,18} The high signal intensity within the tortuous vessels on SE T2-weighted sequences was diagnostic of a low-flow malformation and is attributed to stagnant blood in these abnormal vascular spaces resulting in saturation of protons within the slice.^{17,18} In contrast, normal flow within blood vessels, such as the cephalic vein, appear as a signal loss on SE sequences due to time-of-flight effects because flowing blood is not exposed to both 90° and 180° radiofrequency pulses.¹⁹ The signal loss due to time-of-flight effects is greater at higher velocities, and as a result, all high-flow malformations display large flow voids on SE sequences.^{3,17-19} Thus, venous malformations are usually easily differentiated from high-flow malformations. Occasionally, signal voids representing low-signal intensity septation, dystrophic calcifications or phleboliths can be observed in venous malformations on SE sequences.^{2,10,12,17} In our dog, CT allowed the identification of phleboliths as mineral attenuating foci, which confirmed that the rounded luminal signal voids seen on MRI were phleboliths. Alternatively, a gradient echo T2*-weighted sequence could have been performed to distinguish high-flow high signal intensity versus low-flow, as phleboliths will remain as signal voids.^{12,17}

As demonstrated in this case, CT can screen for high-flow vascular malformations but is of limited use in the investigation of venous malformations because the modality does not clearly delineate the venous vascular pathology.¹²

However, CT does readily allow for assessment of potential phleboliths. Radiography plays a limited role in the diagnostic evaluation of venous malformations due to limited soft-tissue contrast resolution.^{2,12} However, radiography can be a complementary initial screening modality because it allows for the detection of phleboliths in longer standing cases. Radiographically, phleboliths are classically described as radiopacities that are circular or ovoid with a concentric laminated morphology and dense homogeneous mineral or non-uniform mineral centre or uniformly mineral opaque in small phleboliths.^{8,9}

Direct percutaneous venography can help confirm venous malformations in cases that are equivocal on previous imaging modalities.^{2,12} However, venography is generally performed as the initial step within the sclerotherapy procedure to evaluate venous malformation morphology and flow characteristics because venous drainage has an important effect on the efficacy of sclerotherapy.^{12,13,20} Arteriography may be helpful in cases of complex malformations with a high-flow component, but it is not required for the diagnosis and management of low-flow vascular malformations.^{2,12}

Venous malformations do not regress spontaneously and progressively enlarge over time, potentially causing discomfort or dysfunction.²⁰ In people, the indications for treatment of venous malformations include haemorrhage, lesions in life- or limb-threatening location, pain, functional impairment and sepsis.^{13,20} Reported treatment options for venous malformations in people include conservative management, excisional surgery, laser therapy and sclerotherapy, with the latter considered the treatment of choice.^{2,12,13,20} The dog described with a venous malformation in a pelvic limb and presented with swelling and intermittent lameness of the affected limb with perianal and vulvar bleeding was successfully treated with foam sclerotherapy.¹ In contrast to the dog in the other case report, the dog in our case was mostly unaffected by the venous malformation and did not demonstrate apparent discomfort and dysfunction. Although the absence of flow reflects thrombosis and is usually associated with pain in people,¹⁵ the dog in our case was otherwise clinically normal and did not demonstrate signs of pain. Based on the indications outlined for people, the dog in our case did not currently meet the criteria for intervention.^{13,20}

In conclusion, this report illustrates the application of a multimodal imaging approach in the diagnostic investigation and characterisation of a venous malformation with phleboliths in the thoracic limb of a dog. During the investigation of a suspected vascular malformation, imaging studies should be scrutinised for the presence of phleboliths to establish the diagnosis of a venous malformation. Although rare, venous malformation should be considered as a potential differential for multiple, tortuous, subcutaneous blood vessels in a tissue compartment in the dog.

ACKNOWLEDGEMENT

The authors would like to thank Kate Norrie for repeatedly bringing in her dog for imaging procedures. Open access publishing facilitated by Murdoch University, as part of the Wiley - Murdoch University agreement via the Council of Australian University Librarians.

CONFLICT OF INTEREST

The authors have no conflicts of interest to declare.

ETHICS STATEMENT


The authors confirm that the ethical policies of the journal, as noted on the journal's author guidelines page, have been adhered to. The owner of the dog consented to all imaging procedures performed, and there were no experimental procedures performed. Therefore, no ethical committee approval was needed for this case report.

FUNDING INFORMATION

The authors received no specific funding for this work.

ORCID

Kevin Kang  <https://orcid.org/0000-0002-2886-050X>

Robert M. Kirberger  <https://orcid.org/0000-0002-7343-3005>

Giselle Hosgood  <https://orcid.org/0000-0002-8851-8597>

Nerissa Stander  <https://orcid.org/0000-0003-2146-179X>

REFERENCES

- Chang S, Weisse C, Berent AC, Rosen, RJ. Use of percutaneous foam sclerotherapy with 1.5% sodium tetradecyl sulfate for treatment of a pelvic limb venous malformation in a dog. *J Am Vet Med Assoc.* 2020;256(12):1368–74.
- Dubois J, Soulez G, Oliva VL, Berthiaume M, Lapierre C, Therasse E. Soft-tissue venous malformations in adult patients: imaging and therapeutic issues. *RadioGraphics.* 2001;21:1519–31.
- Monroe EJ. Brief description of ISSVA classification for radiologists. *Tech Vasc Interventional Rad.* 2019;22:100628.
- Enjolras O, Ciabrini D, Mazoyer E, Laurian C, Herbreteau D. Extensive pure venous malformations in the upper or lower limb: a review of 27 cases. *J Am Acad Dermatol.* 1997;36:219–25.
- Mazoyer E, Enjolras O, Laurian C, Houdart E, Drouet L. Coagulation abnormalities associated with extensive venous malformations of the limbs: differentiation from Kasbah-Merritt syndrome. *Clin Lab Haem.* 2002;24:243–51.
- Mazoyer E, Enjolras O, Bisdorff A, Perdu J, Wassef M, Drouet L. Coagulation disorders in patients with venous malformation of the limbs and trunk. *Arch Dermatol.* 2008;144(7):861–7.
- Hein KD, Mulliken JB, Kozakewich HPW, Upton J, Burrows PE. Venous malformations of skeletal muscle. *Plast Reconstr Surg.* 2002;110(7):1625–35.
- Eivazi B, Fasnula AJ, Güldner C, Masberg P, Werner JA, Teymoortash A. Phleboliths from venous malformations of the head and neck. *Phlebology.* 2013;28:86–92.
- O'Riordan B. Phleboliths and salivary calculi. *Brit J Oral Surg.* 1974;12:119–31.
- Holloway A, Donaldson D, Kafarnik C. Thrombosed orbital varix in a dog. *Vet Radiol Ultrasound.* 2015;56(5):E58–64.
- Mulliken JB, Glowacki JG. Hemangiomas and vascular malformations in infants and children: a classification based on endothelial characteristics. *Plast Reconstr Surg.* 1982;69(3):412–20.
- Legiehn GM, Heran MKS. Venous malformations: classification, development, diagnosis, and interventional management. *Radiol Clin N Am.* 2008;46:545–97.
- Legiehn GM, Heran MKS. A step-by-step practical approach to imaging diagnosis and interventional radiologic therapy in vascular malformations. *Semin Intervent Radiol.* 2010;27:209–31.
- Paltiel HJ, Burrows PE, Kozakewich HPW, Zurakowski D, Mulliken JB. Soft-tissue vascular anomalies: utility of US for diagnosis. *Radiology.* 2000;214:747–54.
- Trop I, Dubois J, Guibaud L, Grignon A, Patriquin H, McCuaig C, et al. Soft-tissue venous malformations in pediatric and young adult patients: diagnosis with Doppler US. *Radiology.* 1999;212:841–5.
- Ahuja AT, Richards P, Wong KT, Yuen EHY, King AD. Accuracy of high-resolution sonography compared with magnetic resonance imaging in the diagnosis of head and neck venous vascular malformations. *Clin Radiol.* 2003;58:869–75.

17. Flors L, Leiva-Salinas C, Maged IM, Norton PT, Matsumoto AH, Angle JF, et al. MR imaging of soft-tissue vascular malformations: diagnosis, classification, and therapy follow-up. *RadioGraphics*. 2011;31:1321–40.
18. Rak KM, Yakes WF, Ray RL, Dreisbach JN, Parker SH, Luethke JM, et al. MR imaging of symptomatic peripheral vascular malformations. *Am J Roentgenol*. 1992;159:107–12.
19. Westbrook C, Talbot J. *MRI in practice*. 5th ed. Chichester, West Sussex: John Wiley & Sons Ltd; 2019.
20. Burrows PE. Endovascular treatment of slow-flow vascular malformations. *Tech Vasc Interventional Rad*. 2013;16:12–21.

How to cite this article: Kang K, Kirberger RM, Hosgood G, Stander N. Computed tomographic, ultrasonographic, MRI and radiographic findings of a venous malformation with phleboliths in the thoracic limb of a dog. *Vet Rec Case Rep*. 2022;10:e347. <https://doi.org/10.1002/vrc2.347>